Preprint version of a paper published by IMechE in Proc IMechE Part J: J Engineering Tribology (2025) Vol. 239(9) 1246–1257
https://doi.org/10.1177/13506501251349355

Tribofilm Printing of ZDDP and APTES Using Sliding Interfaces

A. Al Sheikh Omar[a*], K. Ahmadi[a], A. P.S Lodhi[a], C. Wang[a], K.J Kubiak[a], A. Morina[a]

[a] *University of Leeds, School of Mechanical Engineering, Institute of Functional Surfaces, Leeds, UK*

Corresponding author: menaals@leeds.ac.uk [a*]

Abstract

The tribo-chemical reactions at the sliding interfaces have proposed an alternative perspective of tribology that can be used in new applications such as electromechanical systems. The single asperity contacts using Atomic Force Microscopy (AFM) and lithography patterning methods have been applied to print 3D film on the surface. However, the drawbacks of these methods are complexity, time, and cost. Therefore, this study will focus on using multi-asperities sliding contacts to print 3D film on contact surfaces. This provides an interesting notion of employing tribology to create film for micro/nanoelectromechanical systems (MEMs/NEMs), through a tribo-chemical process. This study demonstrated the printing of films over steel substrates using the ball-on-disc tribometer (MTM). Zinc Dialkyl Dithiophosphate (ZDDP) and 3-Aminopropyl triethoxysilane (APTES) additives were used as tribo-printable materials. Different test conditions were conducted to build up tribofilm on a steel surface without wear or damage for the substrate. The results confirmed the ability to print thick tribofilm using both materials on steel surfaces. The Energy Dispersive X-Ray (EDX) analysis revealed the formation of ZDDP and APTES tribofilms on the substrate. The Transmission Electron Microscopy (TEM) cross-section technique identified the tribofilm thickness. The film thickness of APTES reached up to 300 nm compared to 100 nm of ZDDP tribofilm without damaging the contact surface. The AFM analysis measured the conductivity of the APTES tribofilm compared to the ZDDP tribofilm which is non-conductive.

Keywords
Tribofilm, 3d printing, ZDDP, APTES, wear

1. Introduction

Several studies [1], [2], [3] have explored the manufacturing of tribofilm that formed during the tribological process to functionalise the surface for small electronic devices that require high precision. The tribofilm in these applications can play a crucial role in protecting the surface, reducing friction, and providing conductivity for electric components in small sizes [4]. The small electronic devices include gyroscopes, nozzles, bio/chemical sensors, micro relays, pressure sensors, microchips, rotation sensors, accelerometers and nanotube-based devices [5], [6], [7], [8], [9]. Some of these electronic devices contain moving parts in the microscale that are difficult to use traditional

lubrication systems. Therefore, the manufacturers of these electric components are interested in improving tribological properties and functionalising the surface without lubricating the contact areas.

The lithography patterning technique is the most common method to fabricate conductive electronic circuits in real applications [10], [11]. The lithography method applies the focused electron beam on targeted materials to promote chemical reactions to fabricate film on the surface. This method is used to build up the conductive film on flexible and rigid substrates [10], [11], [12]. Recently, another method has been introduced to build up tribofilm using the tribology approach. The atomic force microscope (AFM) method has been explored as an alternative method to fabricate patterns on the surface [1], [2], [3]. The AFM technique was used to print 3D tribofilm using single-asperity contacts. Dorgam et al [3] reported a novel method of using AFM to print ZDDP and MoDTC tribofilms (≈100 nm) on silicon and steel substrates. The study was conducted successfully to build up the formed tribofilms under varied test conditions. Gosvami et al.[2] studied several mechanisms that influence the growth of ZDDP tribofilm under sliding contacts of AFM single asperity. The growth rate of tribofilm was correlated to the sliding cycles, contact pressure, and temperature. However, the complexity, time, and cost of the lithography and AFM techniques are still the drawbacks and limitations of film manufacturing for electronic circuits.

The ZDDP has been used in lubricants as a staple antiwear additive due to its performance and the effectiveness of building up anitwear film reducing wear [13], [14], [15], [16], [17], [18], [19]. The ZDDP decomposes and interacts with contact interfaces to grow a protective tribofilm under high temperature and contact pressure [13], [15], [16]. In recent years, ZDDP has been used as Ink for printing 3D film on the surface [1], [3]. The printed film of polyphosphates due to the decomposition of ZDDP results thick film of 100 nm. ZDDP film excels in mechanical and thermal properties to be an ideal additive for 3D printing technology [20]. The drawbacks of ZDDP are a nonfriendly environment and toxic additives due to the existence of sulfur and phosphorus. In addition, ZDDP tribofilm is found to be a nonconductive film [1], [3]. To functionalise the printed ZDDP tribofilm, Duston et al. [1] integrated to graphene nanoplatelets to ZDDP additives. As a result, the carbon-rich layer was formed above the pure ZDDP layer enhancing the tribofilm conductivity [1]. In this study, an alternative material has been explored to replace the ZDDP additive with a polymer-based compound.

Polymer-based compounds have been used in some applications to form self-assembled monolayers [21], [22], [23], [24], [25]. For example, the 3-Aminopropyltriethoxysilane (APTES), a self-assembled monolayer, reacts chemically to the contact surfaces to generate a bonded tribofilm [22], [23], [24], [25]. The APTES has been added to the lubricant formulation to improve the dispersion of

nanoparticles within the lubricants. APTES in the lubricant formulation is considered an environmental safety additive and nontoxic material [26]. Hafeez et al. [26] revealed the formation of the APTES layer on the intrinsic silicon (i-Si). The APTES layer was deposited on the Si substrate using plasma-enhanced chemical vapor deposition (PECVD). The chemical structure of the APTES layer revealed the existence of −Si, −C=O, and −NHS functional groups. The APTES thin layer was formed to enhance the efficiency of solar cells. Miranda et al. [27] applied salinization to deposit APTES thin film on the silicon oxide substrate. Han et al. [28] produced monolayer and non-uniform of multilayer films of APTES on the surface using the silanization method, the thickness of the APTES layer was correlated to the silanization time [28]. However, APTES has not been investigated before as antiwear additive to form protective tribofilm on the rubbing area.

This study aims to develop a conductive and friendly environment film using multi-asperities sliding contacts for small electronic applications. ZDDP additives were exercised as ink to print up tribofilm through AFM signal asperity contact. However, the limitations of AFM-based film printing and other methods such as lithography patterning are the cost, time and complexity. To address these issues, this work introduces an alternative approach that focuses on printing up tribofilm utilizing new printable ink (APTES) and film printing method.

2. Materials and methods

2.1 Materials

The Polyalphaolefin (PAO4) oil was utilized in this study as a solvent with two different additives of ZDDP and APTES. Two mixtures of inks were prepared for this study; the first sample is PAO+10 wt.% ZDDP and the second sample is PAO+10 wt.% APTES. The concentration of 10 wt.% was selected to ensure sufficient additives for printing a thick film on the surface. The APTES (3-Aminopropyltriethoxysilane $C9H23NO3Si$) was purchased from Sigma Aldrich, UK. The molecular structure of APTES and its reactions with the metal surface are represented in Figure *1*a, b. The APTES compound contains three metal reactive groups (ethoxysilane) as shown in Figure *1*a. The hydroxyl groups from ethoxysilane react with the metal surface through the chemisorption process to form a monolayer (Figure *1*b) [29].

Preprint version of a paper published by IMechE in Proc IMechE Part J: J Engineering Tribology (2025) Vol. 239(9) 1246–1257
https://doi.org/10.1177/13506501251349355

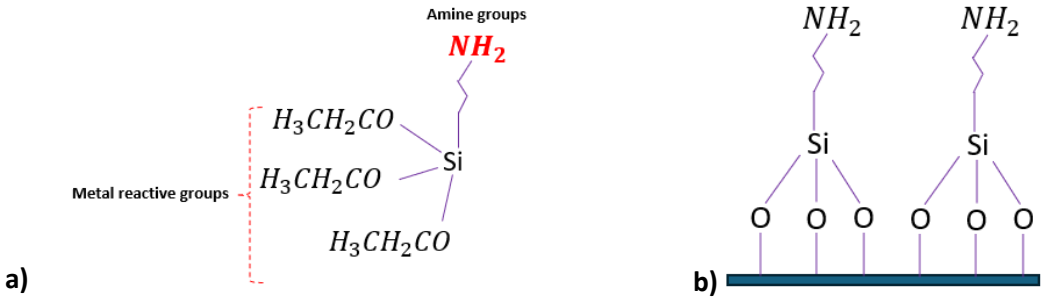

Figure 1: a) Schematic representations of the chemical structure of APTES, b) APTES reactions with the metal surface to form the monolayer.

2.2 Tribological test

MTM tribometer was conducted to run tribological tests as shown in Figure *2*. The material properties of the ball and disc and test conditions are reported in Table 1. The test conditions are selected with two different entrainment speeds 500 and 2000 mm/s to create two different contact regimes. The contact interfaces are in boundary with a lower speed (Lambda λ= 0.6 < 1) and hydrodynamic regime with a higher speed (Lambda λ= 1.7 < 1). The maximum contact pressure was 0.53 GPa. The MTM tests are repeated at least two times to ensure the repeatability of tests.

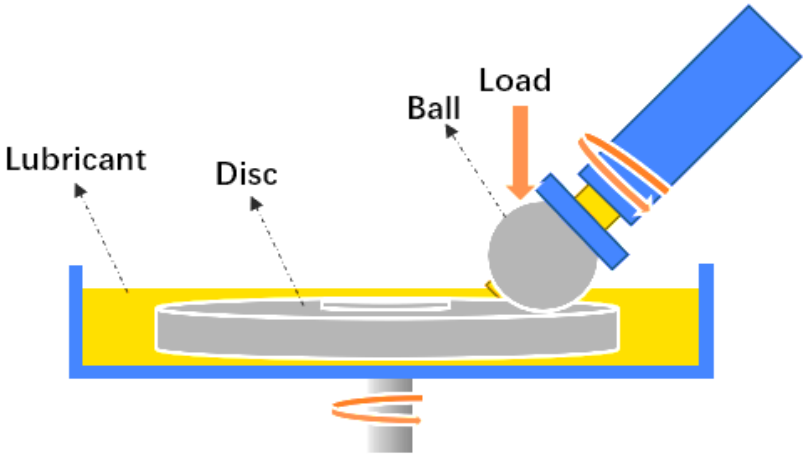

Figure 2: Contact interfaces using MTM tribometer.

Table 1: Tribological test conditions and material properties of MTM specimens.

Parameters	Values	Details	MTM ball	MTM disc
Load (N)	5	**Material**	steel	steel
Temperature (C°)	70	**Elastic modulus (GPa)**	207	207
Slide-roll ratio (SRR) %	200	**Poisson's ratio**	0.3	0.3
Duration (mins)	60	**Roughness, Ra (nm)**	9	185

Entrainment speed (mm/s)	500,2000	**Diameter (mm)**	19.05	46
Lambda ratio (λ)				
Max contact pressure (GPa)	0.53			

2.3 Post-surface analysis

An optical white light interferometer (NPFLEX) is conducted to analyse the surface after tribological tests. The surfaces of MTM discs are scanned across the wear rubbing area by NFLEX and the obtained images were processed using vision64 software from Burker Ltd, USA. Moreover, the surface analysis of the wear scar of MTM discs was carried out using the Scanning Electron Microscopy (SEM) technique. The SEM analysis can provide high-resolution images of the surface damage and tribofilm formation on the rubbing area. Energy Dispersive X-ray (EDX) analyser was conducted to detect the chemical composition of the printed tribofilm on the MTM disc. The conductivity of the printed tribofilms for two different additives ZDDP and APTES was carried out using conductive atomic force microscopy (CAFM, Bruker, USA). The scanning area of 0.5 x 2 μm^2 inside the rubbing area was conducted with a resonant frequency of 2 kHz, a nominal spring constant of 40 N/m, a speed of 40 $\mu m/s$, a low contact force of 45 nN and a scanning angle of 90°. CAFM function was used to apply a voltage across the contact area of the SCM-PIC-V2 tip and the scanned area. As a result, a current flow can be recorded simultaneously with topography images of the scanned area. This arrangement allows us to measure the topography and conductivity of the printed tribofilms.

2.4 Film cross-section analysis using Transmission Electron Microscopy/Focussed Ion Beam (FIB)

The internal structure of printed tribofilm, which was produced from two different inks, was analysed using the TEM-FIB technique. The FIB (FEI Helios G4 CX Daul beam) was conducted to create a slice on the printed tribofilm. The cross-section of tribofilms was analysed using TEM/EDX (FEI Titan Themis 300) mapping to observe the thickness and elemental distribution of the tribofilms.

3. Results and discussion

3.1 Friction

The tribological tests of two different lubricants of PAO+10 wt% ZDDP and PAO+10 wt% APTES were carried out at two different entrainment speeds. The friction results are reported in Figure 3. For the PAO+10 wt% ZDDP oil sample (Figure 3a), the friction coefficient starts high at the first 10 mins of running the test (running-in period) and stabilises to the end of the test. At the end of tribological tests, the average friction coefficient at a low speed of 500 rpm is approximately 0.11 compared to 0.07 the friction coefficient for a higher speed of 2000 rpm.

For the PAO+10 wt% APTES oil sample (Figure 3b), the friction coefficient begins high initially and decreases over time until the end of the tribological test. The high and fluctuating friction coefficient observed for the APTES oil sample at low speed is probably due to stick and slip behaviour. The friction coefficient for APTES oil samples at high speed shows a lower and constant friction coefficient over the test compared to high speed. The average friction coefficient at 500 rpm speed is approximately 0.2 compared to 0.06 at 2000 speed. At the high speed of APTES lubricant, a more stable and lower friction coefficient was observed due to the smooth transition from stick to slip.

The comparison of friction performance for ZDDP and APTES at the speed of 2000 rpm is shown in Figure 3a,b. The results indicate a lower friction coefficient (μ=0.06) of APTES compared to the ZDDP oil sample (μ=0.07). The reduction of friction of two lubricant samples at high speed (2000 rpm) is due to changing the lubrication regimes from boundary to mixed regime. This agrees with previous studies [30], [31] revealing the effect of rotation speed on reduction in the friction coefficients.

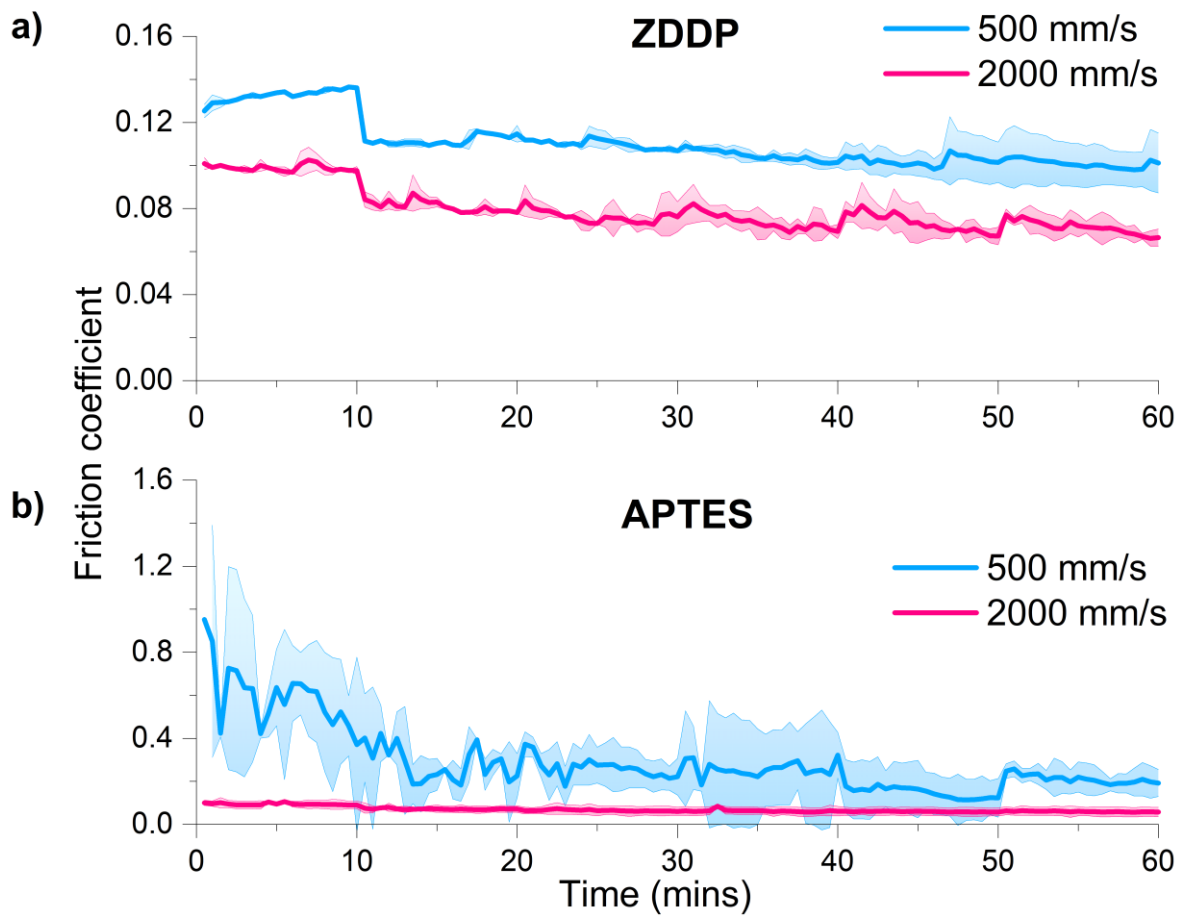

Figure 3: Friction results of PAO+10 wt% ZDDP (a) and PAO+10 wt% APTES (b) at different speeds of 500 and 2000 mm/s.

3.2 Surface analysis of sliding interfaces

Surface analysis using NPFLEX for the MTM discs was performed to investigate the surface damage or wear in the sliding interfaces of the wear track. The 3d surface images combined with the surface profiles of the scanned surfaces are reported in Figure 4. The surface images (Figure 4a,b and d) indicate no damage caused after the tribology test for all oil samples excluding the PAO + 10wt% APTES sample at a speed of 500 rpm (Figure 4c). The surface images contain some scratches on the surface originating from sample manufacturing, an example shown in Figure *4*a. The wear profile of the PAO + 10wt% APTES oil sample at low speed demonstrates material losses from the wear track as shown in Figure 4c. The surface analysis of rubbing areas of the tests PAO + 10wt% ZDDP (at 500, 2000 rpm) and PAO + 10wt% APTES (at 2000 rpm) shows no noticeable damage observed. This suggests the formation of a protection layer on the surface acts as a lubrication film reducing the wear and friction. Further SEM-EDX analysis in this section will examine the presence or absence of the deposited tribofilm in the contact area, providing initial evidence of the distribution and composition of expected printed films.

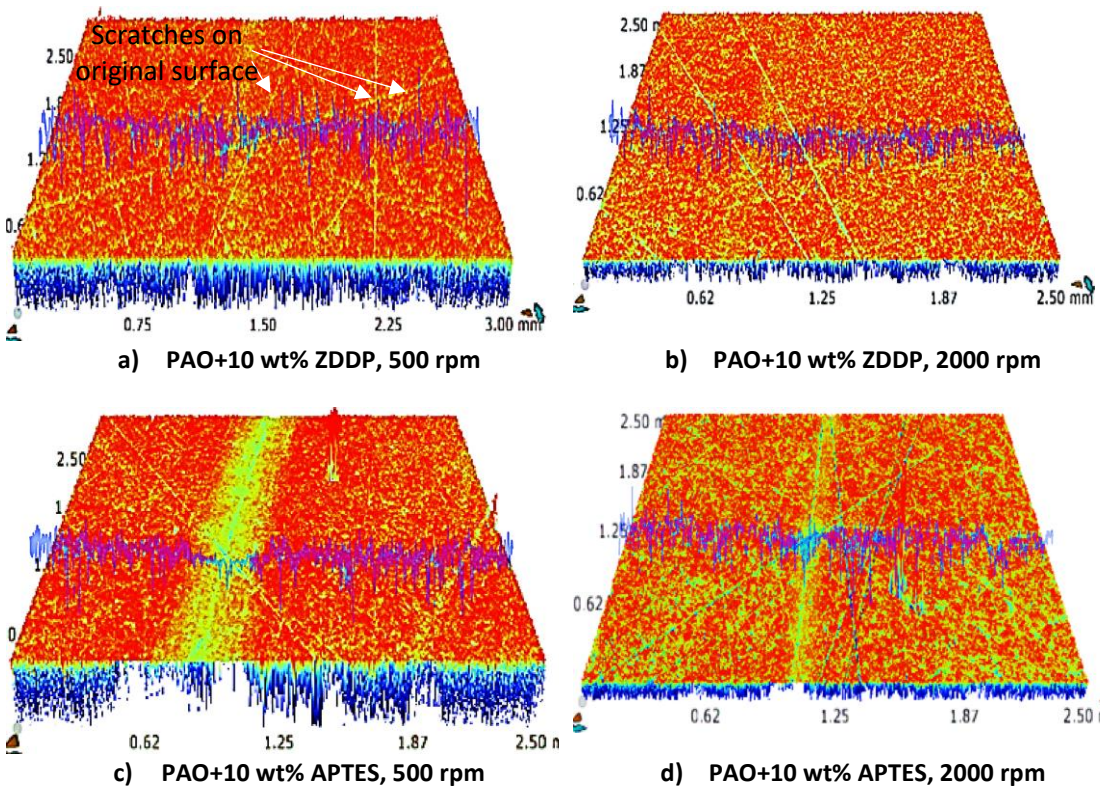

Figure 4: NPFEX surface analysis for MTM discs for oil samples at end of tribological tests a) PAO+10 wt% ZDDP at a speed of 500 rpm, b) PAO+10 wt% ZDDP at a speed of 2000 rpm, c) PAO+10 wt% APTES at a speed of 500 rpm, d) and d) PAO+10 wt% APTES at speed of 2000 rpm.

Preprint version of a paper published by IMechE in Proc IMechE Part J: J Engineering Tribology (2025) Vol. 239(9) 1246–1257
https://doi.org/10.1177/13506501251349355

The SEM/EDX analysis was conducted for all tested samples inside and outside the wear track of sliding contacts to investigate the existence of tribofilm, demonstrated in Figure 5. Surface analysis of PAO + 10 wt% ZDDP lubricant at a speed of 500 rpm is presented in Figure *5*a. The results reveal no damage or lost materials in the contact area apart from the scratches from the original surface sample. The dark area on the surface represents the sliding area of interface contacts. Chemical analysis using EDX inside and outside the wear track was performed as shown in Figure *5*a_1. Figure *5*a_1 shows the existence of ZDDP tribofilm elements (Zn, S, and P) identified in spectrum 1, compared to the absence of the tribofilm elements outside the wear track in spectrum 2. The absence of significant damage on the interface area with the presence of ZDDP key elements from the ZDDP additive indicates the successful deposition of ZDDP film on the surface. A similar SEM/EDX analysis was carried out for PAO + 10 wt% ZDDP at a speed of 2000 rpm, illustrated in Figure *5*b, b_1. The main observation is no damage on the contact surface. The EXD data confirms the presence of ZDDP elements (Zn, S, and P) inside the wear track, with a slightly higher elemental concentration compared to the same sample conducted at a lower speed as shown in Figure *5*a_1,b_1. It is important to highlight that SEM/EDX for this sample was carried out after TEM-FIB analysis. This can explain the existence of the Pt element in the spectra, which comes from the sample preparation process.

For the oil sample of PAO + 10 wt% APTES at a speed of 500 rpm, the surface analysis of sliding contacts shows no wear or damage. APTES tribofilm (darker colour) was observed on the sliding area as shown in Figure *5*c. Chemical analysis of APTES tribofilm indicates the increase in the elemental concentration of C, Si, and O inside wear track compared to the outside wear track (Figure *5*c_1). Similar findings for the PAO + 10 wt% APTES at a speed of 2000 rpm were observed in (Figure *5*d, d_1). Higher C, Si, and O concentrations were noticed for the APTES oil sample at 2000 rpm compared to the sample at lower speed (500 rpm). This observation can support the friction data in Figure *3*b which shows a stable coefficient of friction due to dense deposited film on the surface reducing friction.

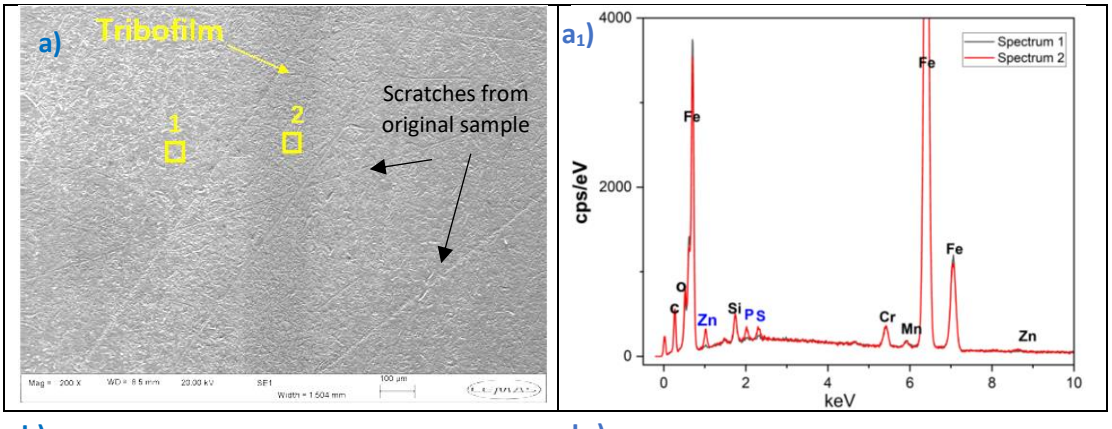

b) b_1)

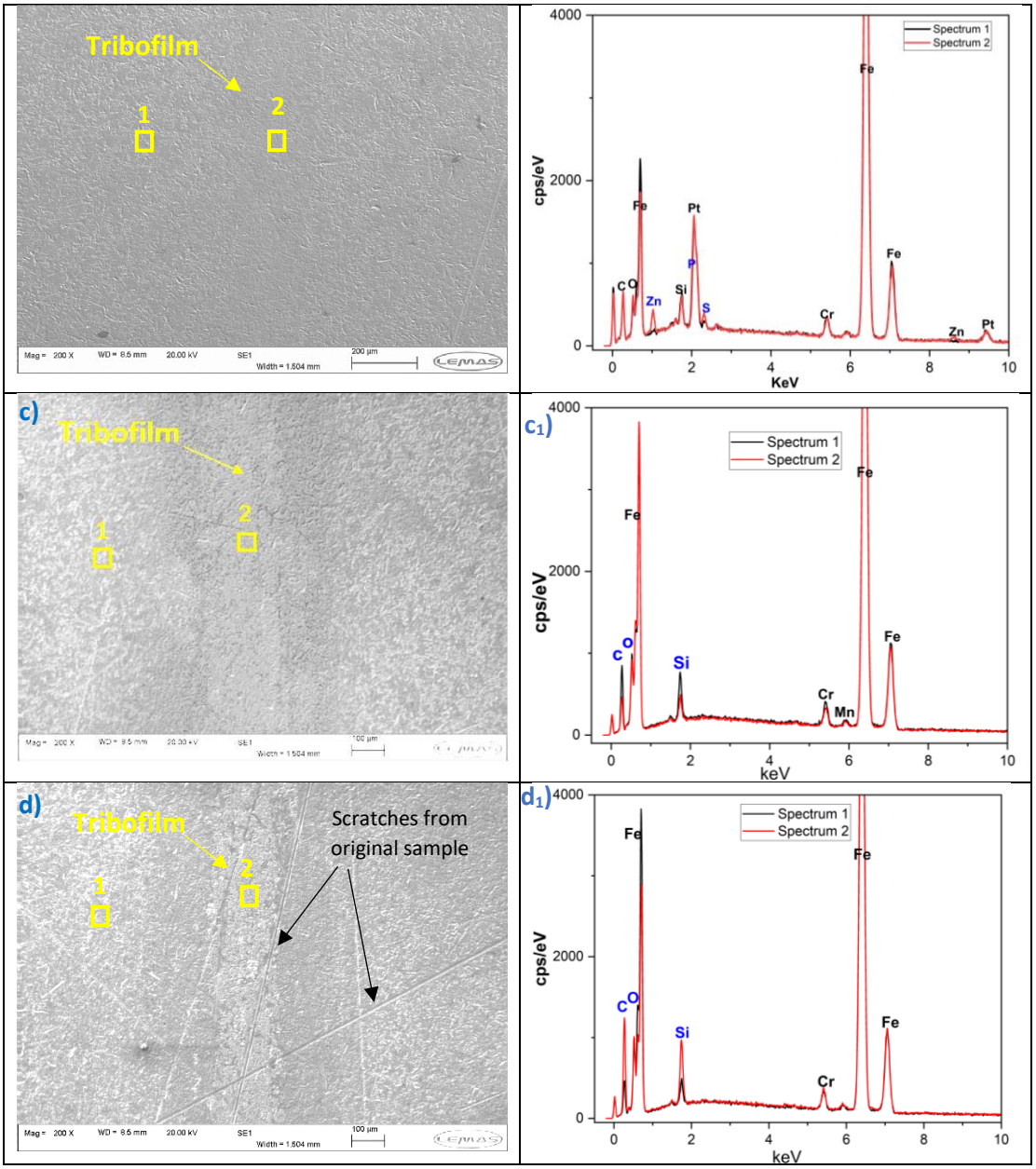

Figure 5: SEM/EDX analysis for sliding contacts and outside the rubbing area a) a_1) SEM image and EDX data for the PAO+10 wt% ZDDP, 500 rpm test, b) b_1) SEM image and EDX data for the PAO+10 wt% ZDDP, 2000 rpm test, c) c_1) SEM image and EDX data for the PAO+10 wt% APTES, 500 rpm test d) d_1) SEM and EDX data for the PAO+10 wt% APTES, 2000 rpm test.

3.3 Cross-section analysis of printed tribofilm

The SEM-EDX analysis confirmed the existence of the ZDDP and APTES tribofilms printed on the substrate by analysing the distribution of tribofilm elements, as reported in Figure 5. The chemical analysis using TEM cross-section provides insights into the detailed mapping of nanostructure across printed films. The spatial resolution of TEM-EDX for ZDDP tribofilm shows the distribution of Zn, S, P, C, and O elements throughout the tribofilm section (Figure 6). The TEM-EDX results do not detect any iron across the film section which confirms no wear debris from the surface existed inside the film. The tribofilm maps report that the inner layer, which adheres to the iron surface with a thickness of <

10 nm, is rich in S, O, and C-based compounds (Figure 6). The external layer comprises Zn, P, S, O, and C-based compounds. Shimizu et al.[32] found the formation of sulphur-rich tribofim initially and Zn/P based layers were developed over test time. These primary elements that contribute to the formation of ZDDP anitwear film are investigated in the chemical analysis of tribofilm cross-section. These elements come from complex and different structured layers formed on the metal surface minimizing the wear [15], [16], [33], [34].

This is in parallel line with previous studies [16], [33], [35] that investigate the hypothesis of ZDDP tribofilm formation steps. The ZDDP tribofilm formation can be divided into the following steps starting with the adsorption of ZDDP molecules into the metal surface, the decomposition of ZDDP molecules, the formation of an initial layer of the mixture of oxide/sulfates/sulfide, and finally the formation of Zn/Fe polyphosphates over the rubbing time [15], [16], [33], [34].

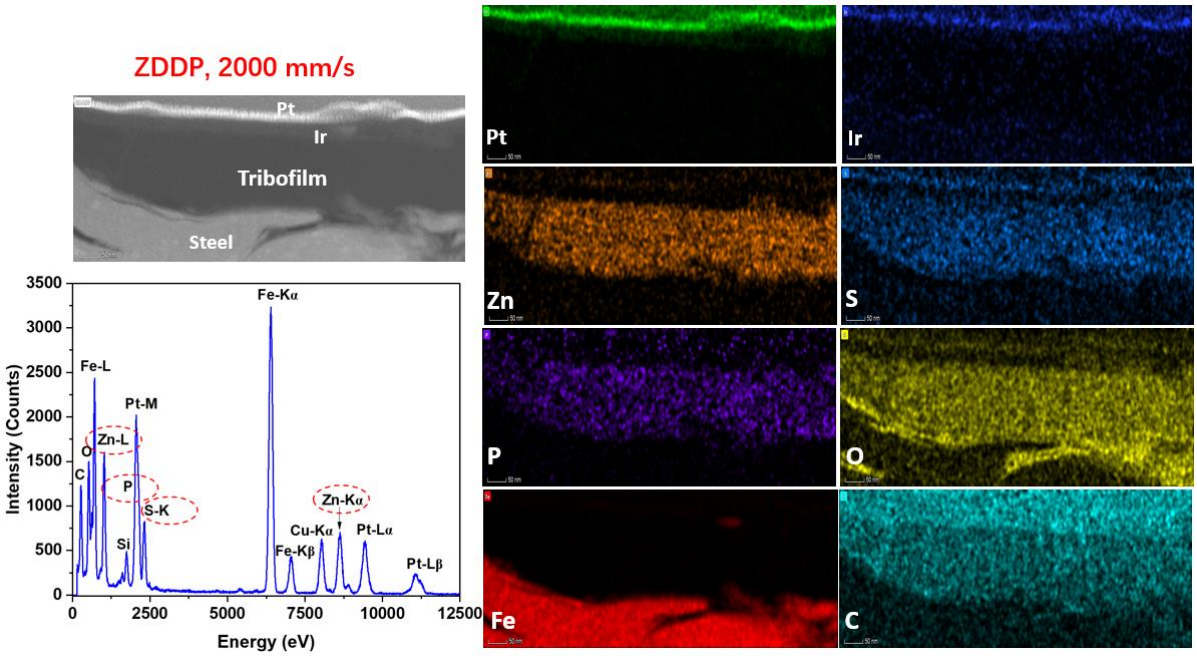

Figure 6: Chemical analysis of ZDDP tribofilm on the MTM disc using TEM-FIB for the PAO + 10 wt% ZDDP, 2000 rpm sample.

The chemical analysis across the depth profiling of APTES tribofilm is presented in Figure 7. The TEM-EDX of APTES tribofilm reveals the presence of three primary elements C, Si, and O. The APTES layer, which adheres to the steel substrate, is mainly rich with C, Si, and O-based compounds.

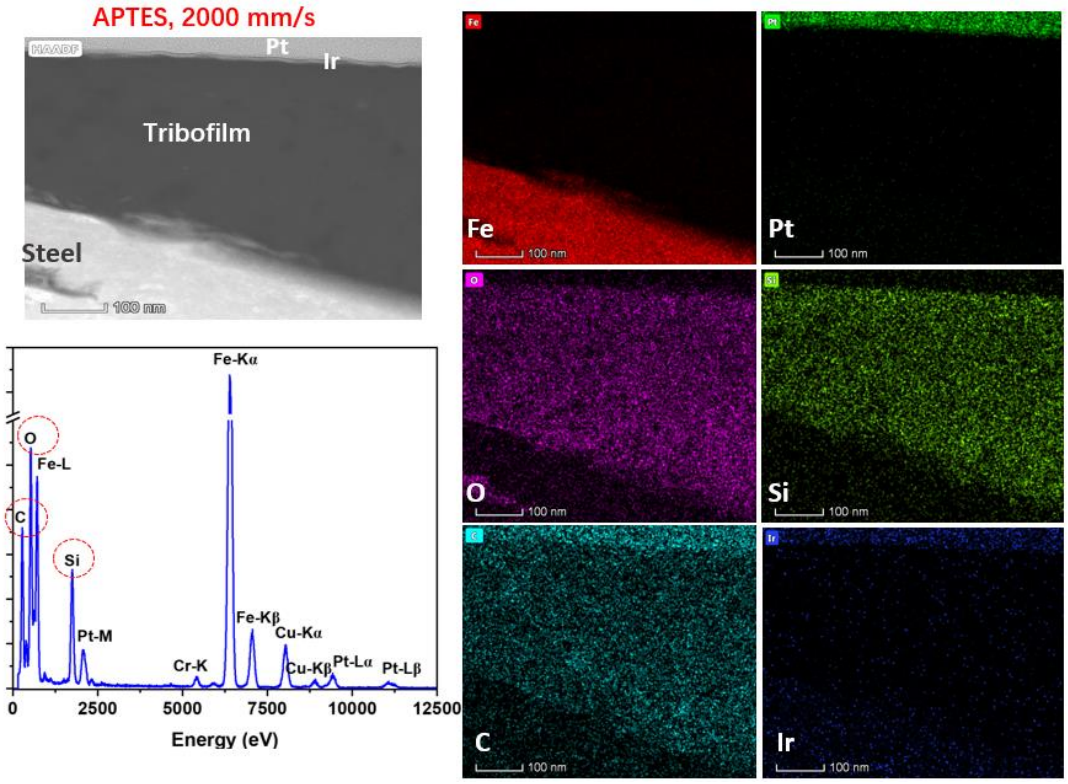

Figure 7: Chemical analysis of APTES tribofilm on the MTM disc using TEM-FIB for the PAO + 10 wt% APTES, 2000 rpm sample.

The TEM-FIB technique was used in this study to evaluate the thickness of ZDDP and APTES tribofilms. The PAO + 10 wt% ZDDP lubricant at a speed of 500 rpm demonstrates the tribofilm thickness of ≈60 nm as shown in Figure 8a. At the higher speed of 2000 rpm, the PAO + 10 wt% ZDDP oil reveals higher tribofilm thickness, approximately 100 nm (Figure 8b). In this study, a notable impact on the ZDDP tribofilm thickness was identified at the speed of 2000 rpm with pure sliding. This is due to the increase of the sliding distance over running time leading to thicker tribofilm [2]. In comparison, the PAO combined with 10 wt% APTES lubricant at a lower speed of 500 rpm produces APTES tribofilm with a thickness of ≈40 nm (Figure 8c). At a higher speed of 2000 rpm, the APTES tribofilm thickness significantly increased to ≈300 nm, as illustrated in Figure 8d.

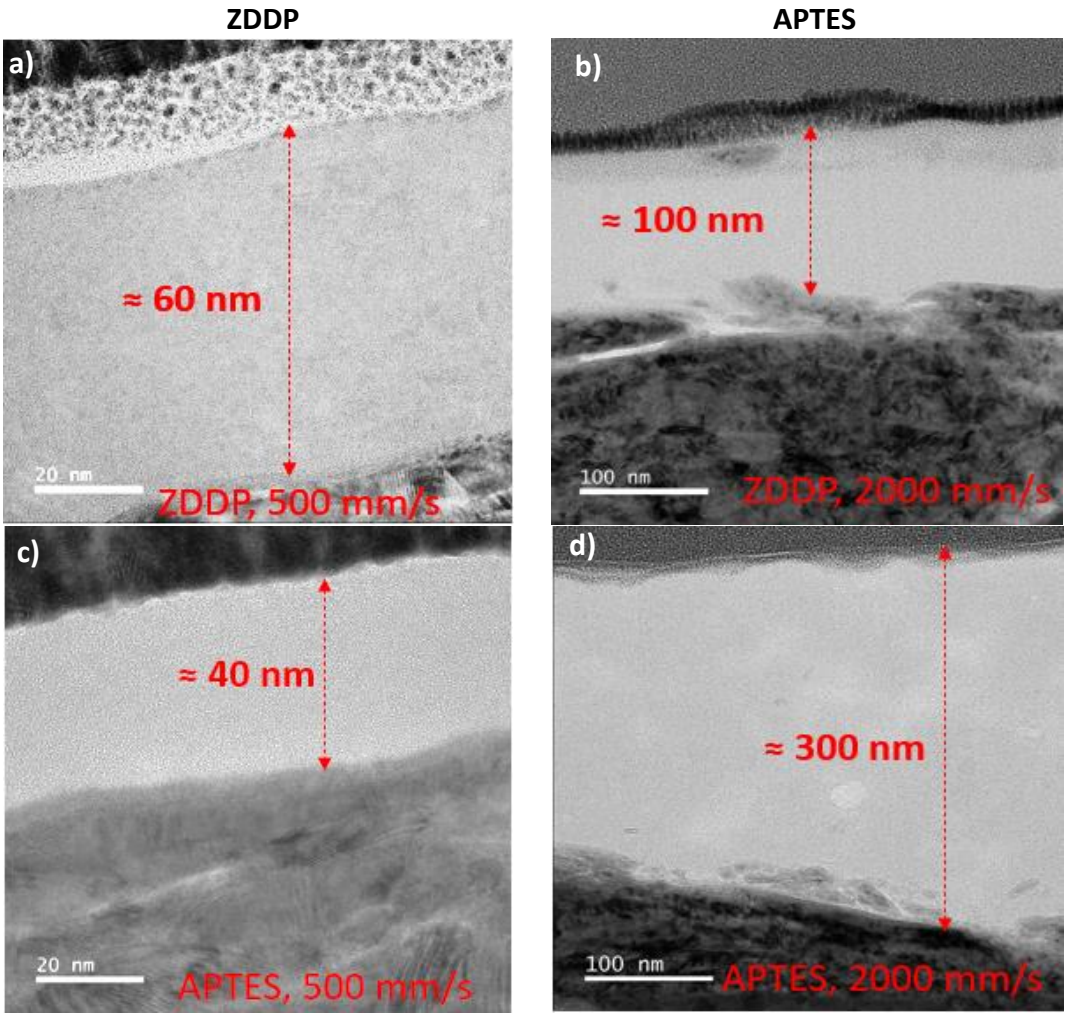

Figure 8: TEM-FIB cross-section of tribofilm images for the following samples a) PAO + 10 wt% ZDDP, 500 rpm, b) PAO + 10 wt% ZDDP, 2000 rpm, c) PAO + 10 wt% APTES, 500 rpm, d) PAO + 10 wt% APTES, 2000 rpm.

The authors propose the following mechanism of the APTES formation layer, illustrated in Figure *9*. APTES self-assembled monolayer forms due to chemical interactions of ethoxysilane groups with the contact surfaces resulting in a thin APTES monolayer (Figure 9). There is no strong chemical bonding or interaction between the APTES molecules (-NH2 with -NH2 or -NH2 with -H3CH2CO). The growth of APTES multilayers has been reported to be formed [22], [23], [24], [25] due to the gradually accumulating APTES layer. The deposition and condensation of the APTES layer can be influenced by partially hydrolysed APTES or mechanical action [22], [23], [24], [25].In this study, as the tribological test starts, more APTES molecules are deposited physically on the surface due to mechanical action

(sliding and rolling) (Figure 9). As a result, a thicker and more stable protection layer is formed on the rubbing area compared to outside the interface contacts enhancing the tribological performance.

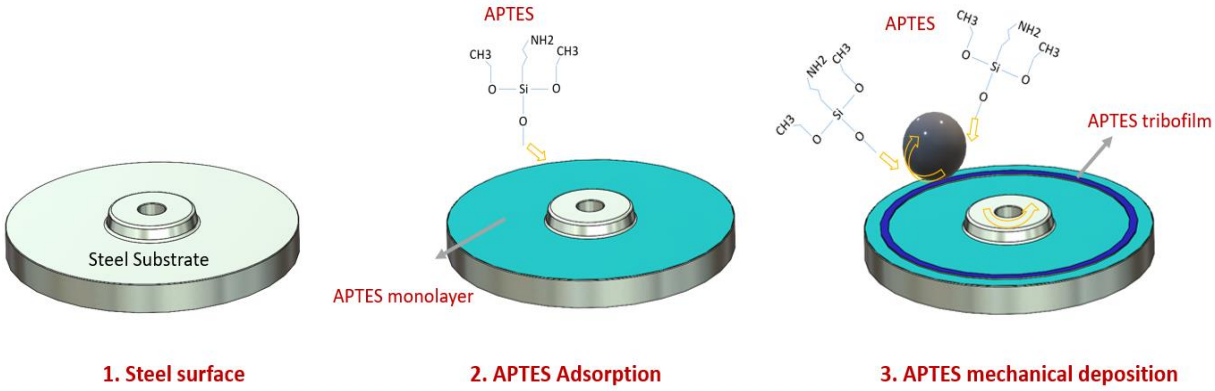

Figure 9: 3D schematic explains the mechanism steps of APTES tribofilm printing.

3.4 Tribofilm conductivity

The conductivity of ZDDP and APTES tribofilms has been carried out using AFM (C-AFM). The scanned area of disc samples in the wear track is 0.5*2 μm^2. The topography and conductivity of ZDDP and APTES tribofilms are illustrated in Figure 10. This was done by measuring the current through the AFM tip and the AFM tip deflection. The topography of ZDDP tribofilm as shown in Figure 10a demonstrated the existence of ZDDP tribofilm covering the halved image (bottom side). In the Figure 10b shows the tribofilm is not conducive in the area that is covered by ZDDP tribofilm. In the topography image (Figure 10a), where is not covered by ZDDP tribofilm (top side), the current passes through the steel substrate. The results align with the previous study [1] that revealed nonconductive ZDDP tribofilm. To make ZDDP film conductive, Dustan et al. [1] combined ZDDP with a high concentration of graphene nanoparticles to form ZDDP film-rich carbon.

The topography and conductivity of APTES tribofilm are illustrated in Figure 10c,d. Figure 10c shows that ATPES tribofilm covers mostly the whole scanned surface. In parallel measurement, Figure 10d reveals that the current passes through the APTES tribofilm to the steel substrate. Some scanned areas, in Figure 10d where there is no APTES tribofilm, are nonconductive surfaces. This could be due to the coverage of the contamination or oxidation for non-APTES coverage areas over the steel surface, preventing the current access through the steel substrate. The APTES tribofilm mainly consists of silicon/carbon-rich film, demonstrated in Figure *7*, which helps APTES to be conductive compared to ZDDP tribofilm.

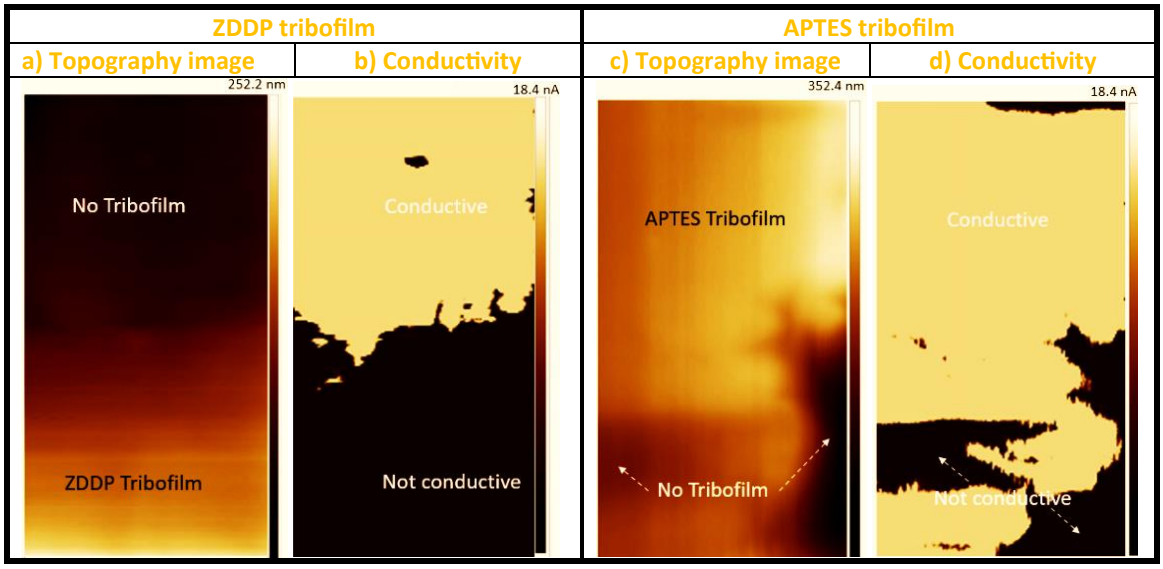

Figure 10: The topography and conductivity of ZDDP and APTES tribofilms.

4. Conclusions

In this study, printing tribofilm for the MEMs/NEMs applications has been investigated using new printing method and ink. Multi-asperity contact surface using the MTM tribometer was conducted. Two different printable materials including ZDDP and APTES were used to build up tribofilms on the steel surface. The main conclusions are:

- 3D tribofilm was successfully printed using the multi-asperity contact method without any wear or damage on the substrate.
- The MTM test conditions were selected to print up the tribofilms at different lubrication regimes.
- Both printable inks of ZDDP and APTES were used to print up thick and robust tribofilms.
- Rotation speed affected the formation of tribofilm for both inks, significantly influencing the APTES tribofilm thickness.
- The chemical composition of APTES tribofilm indicated a silicon and carbon-rich tribofilm.
- The ZDDP printed film was nonconductive compared to APTES conductive film.

5. Acknowledgments

6. Declaration of interest statement

7. Declaration of data availability

8. References

[1] S. Duston, R. A. Oliver, K. J. Kubiak, Y. Wang, C. Wang, and A. Morina, 'Tribological manufacturing of ZDDP tribofilms functionalised by graphene nanoplatelets', *JPhys Materials*, vol. 7, no. 4, Oct. 2024, doi: 10.1088/2515-7639/ad6930.

[2] N. N. Gosvami, J. A. Bares, F. Mangolini, A. R. Konicek, D. G. Yablon, and R. W. Carpick, 'Mechanisms of antiwear tribofilm growth revealed in situ by single-asperity sliding contacts', *Science (1979)*, vol. 348, no. 6230, pp. 102–106, Apr. 2015, doi: 10.1126/science.1258788.

[3] A. Dorgham, C. Wang, A. Morina, and A. Neville, '3D tribo-nanoprinting using triboreactive materials', *Nanotechnology*, vol. 30, no. 9, Jan. 2019, doi: 10.1088/1361-6528/aaf70c.

[4] R. L. Jackson, A. B. Coker, Z. Tucker, M. S. Hossain, and G. Mills, 'An Investigation of Silver-Nanoparticle-Laden Lubricants for Electrical Contacts', *IEEE Trans Compon Packaging Manuf Technol*, vol. 9, no. 2, pp. 193–200, Feb. 2019, doi: 10.1109/TCPMT.2018.2887402.

[5] B. Bhushan, 'Nanotribology and nanomechanics of MEMS/NEMS and BioMEMS/BioNEMS materials and devices', *Microelectron Eng*, vol. 84, no. 3, pp. 387–412, Mar. 2007, doi: 10.1016/j.mee.2006.10.059.

[6] A. Arab and Q. Feng, 'Reliability research on micro- and nano-electromechanical systems: a review', *International Journal of Advanced Manufacturing Technology*, vol. 74, no. 9–12, pp. 1679–1690, Oct. 2014, doi: 10.1007/s00170-014-6095-x.

[7] R. Hajare, V. Reddy, and R. Srikanth, 'MEMS based sensors – A comprehensive review of commonly used fabrication techniques', in *Materials Today: Proceedings*, Elsevier Ltd, 2021, pp. 720–730. doi: 10.1016/j.matpr.2021.05.223.

[8] H. Gong, C. Yu, L. Zhang, G. Xie, D. Guo, and J. Luo, 'Intelligent lubricating materials: A review', Dec. 01, 2020, *Elsevier Ltd*. doi: 10.1016/j.compositesb.2020.108450.

[9] C. Chircov and A. M. Grumezescu, 'Microelectromechanical Systems (MEMS) for Biomedical Applications', Feb. 01, 2022, *MDPI*. doi: 10.3390/mi13020164.

[10] I. D. Joshipura, H. R. Ayers, C. Majidi, and M. D. Dickey, 'Methods to pattern liquid metals', Apr. 28, 2015, *Royal Society of Chemistry*. doi: 10.1039/c5tc00330j.

[11] R. Abbasi *et al.*, 'Photolithography-enabled direct patterning of liquid metals', *J Mater Chem C Mater*, vol. 8, no. 23, pp. 7805–7811, Jun. 2020, doi: 10.1039/d0tc01466d.

[12] Y.-M. Lee, 'Introduction to optical lithography', in *Efficient Extreme Ultraviolet Mirror Design*, IOP Publishing, 2021. doi: 10.1088/978-0-7503-2652-0ch1.

[13] G. Pereira *et al.*, 'A variable temperature mechanical analysis of ZDDP-derived antiwear films formed on 52100 steel', *Wear*, vol. 262, no. 3–4, pp. 461–470, Feb. 2007, doi: 10.1016/j.wear.2006.06.016.

[14] L. J. Taylor and H. A. Spikes, 'Friction-enhancing properties of zddp antiwear additive: Part i—friction and morphology of zddp reaction films', *Tribology Transactions*, vol. 46, no. 3, pp. 303–309, Jan. 2003, doi: 10.1080/10402000308982630.

[15] Z. Zhang, E. S. Yamaguchi, M. Kasrai, G. M. Bancroft, X. Liu, and M. E. Fleet, 'Tribofilms generated from ZDDP and DDP on steel surfaces: Part 2, chemistry', *Tribol Lett*, vol. 19, no. 3, pp. 221–229, Jul. 2005, doi: 10.1007/s11249-005-6149-1.

[16] A. Dorgham *et al.*, 'In situ synchrotron XAS study of the decomposition kinetics of ZDDP triboreactive interfaces', *RSC Adv*, vol. 8, no. 59, pp. 34168–34181, 2018, doi: 10.1039/C8RA04753G.

[17] M. Aktary, M. T. Mcdermott, and G. A. Mcalpine, 'Morphology and nanomechanical properties of ZDDP antiwear films as a function of tribological contact time'.

[18] Y. R. Li, G. Pereira, M. Kasrai, and P. R. Norton, 'The effect of steel hardness on the performance of ZDDP antiwear films: A multi-technique approach', *Tribol Lett*, vol. 29, no. 3, pp. 201–211, Mar. 2008, doi: 10.1007/s11249-008-9297-2.

[19] A. Al Sheikh Omar, F. M. Salehi, U. Farooq, A. Neville, and A. Morina, 'Effect of Zinc Dialkyl Dithiophosphate Replenishment on Tribological Performance of Heavy-Duty Diesel Engine Oil', *Tribol Lett*, vol. 70, no. 1, Mar. 2022, doi: 10.1007/s11249-022-01565-8.

[20] W. Feng, H. Song, Z. Lu, ZhiquanYang, and X. Hu, 'On the mechanical and tribological performances of the tribofilm formed by zinc dialkyl dithiophosphate', *Journal of Industrial and Engineering Chemistry*, vol. 122, pp. 152–160, Jun. 2023, doi: 10.1016/j.jiec.2023.02.017.

[21] M. Sypabekova, A. Hagemann, D. Rho, and S. Kim, 'Review: 3-Aminopropyltriethoxysilane (APTES) Deposition Methods on Oxide Surfaces in Solution and Vapor Phases for Biosensing Applications', Jan. 01, 2023, *MDPI*. doi: 10.3390/bios13010036.

[22] A. Simon, T. Cohen-Bouhacina, M. C. Porté, J. P. Aimé, and C. Baquey, 'Study of two grafting methods for obtaining a 3-aminopropyltriethoxysilane monolayer on silica surface', *J Colloid Interface Sci*, vol. 251, no. 2, pp. 278–283, 2002, doi: 10.1006/jcis.2002.8385.

[23] Q. Gu and X. Cheng, 'Tribological behaviors of self-assembled 3-aminopropyltriethoxysilane films on silicon', *Current Applied Physics*, vol. 8, no. 5, pp. 583–588, Aug. 2008, doi: 10.1016/j.cap.2007.10.054.

[24] W. Wang and M. W. Vaughn, 'Morphology and amine accessibility of (3-aminopropyl) triethoxysilane films on glass surfaces', *Scanning*, vol. 30, no. 2, pp. 65–77, Mar. 2008, doi: 10.1002/sca.20097.

[25] E. T. Vandenberg, L. Bertilsson, B. O. Liedberg, K. Uvdal, R. Erlandsson, and H. Elwing, 'Structure of 3-Aminopropyl Triethoxy Silane on Silicon Oxide', 1991.

[26] H. Hafeez *et al.*, 'Replacement of n-type layers with a non-toxic APTES interfacial layer to improve the performance of amorphous Si thin-film solar cells', *RSC Adv*, vol. 9, no. 13, pp. 7536–7542, 2019, doi: 10.1039/C8RA07409G.

[27] A. Miranda, L. Martínez, and P. A. A. De Beule, 'Facile synthesis of an aminopropylsilane layer on Si/SiO2 substrates using ethanol as APTES solvent', *MethodsX*, vol. 7, Jan. 2020, doi: 10.1016/j.mex.2020.100931.

[28] Y. Han, D. Mayer, A. Offenhäusser, and S. Ingebrandt, 'Surface activation of thin silicon oxides by wet cleaning and silanization', *Thin Solid Films*, vol. 510, no. 1–2, pp. 175–180, Jul. 2006, doi: 10.1016/j.tsf.2005.11.048.

[29] S. S. Piletsky, A. G. Cruz, E. Piletska, S. A. Piletsky, E. O. Aboagye, and A. C. Spivey, 'Iodo Silanes as Superior Substrates for the Solid Phase Synthesis of Molecularly Imprinted Polymer Nanoparticles', *Polymers (Basel)*, vol. 14, no. 8, Apr. 2022, doi: 10.3390/polym14081595.

[30] M. Polajnar and M. Kalin, 'Effect of the Slide-to-Roll Ratio and the Contact Kinematics on the Elastohydrodynamic Friction in Diamond-Like-Carbon Contacts with Different Wetting Behaviours', *Tribol Lett*, vol. 60, no. 1, Oct. 2015, doi: 10.1007/s11249-015-0593-3.

[31] C. Quinn *et al.*, 'Experimental investigation of friction in compliant contact: The effect of configuration, viscoelasticity and operating conditions', *Tribol Int*, vol. 165, Jan. 2022, doi: 10.1016/j.triboint.2021.107340.

[32] Y. Shimizu and H. A. Spikes, 'The Influence of Slide–Roll Ratio on ZDDP Tribofilm Formation', *Tribol Lett*, vol. 64, no. 2, Nov. 2016, doi: 10.1007/s11249-016-0738-z.

[33] M. Ueda, A. Kadiric, and H. Spikes, 'On the Crystallinity and Durability of ZDDP Tribofilm', *Tribol Lett*, vol. 67, no. 4, Dec. 2019, doi: 10.1007/s11249-019-1236-x.

[34] A. Dorgham *et al.*, 'In situ synchrotron XAS study of the decomposition kinetics of ZDDP triboreactive interfaces', *RSC Adv*, vol. 8, no. 59, pp. 34168–34181, 2018, doi: 10.1039/C8RA04753G.

[35] A. Dorgham *et al.*, 'Tribochemistry evolution of DDP tribofilms over time using in-situ synchrotron XAS', *Tribol Int*, vol. 160, Aug. 2021, doi: 10.1016/j.triboint.2021.107026.